sustainability

MDPI

Article

Characteristics of Biochars Derived from the Pyrolysis and Co-Pyrolysis of Rubberwood Sawdust and Sewage Sludge for Further Applications

Liaqat Ali [1], Arkom Palamanit [2], Kuaanan Techato [1], Asad Ullah [3], Md. Shahariar Chowdhury [1] and Khamphe Phoungthong [1,*]

[1] Environmental Assessment and Technology for Hazardous Waste Management Research Center, Faculty of Environmental Management, Prince of Songkla University, Songkhla 90112, Thailand; liaqatali.gorshani@gmail.com (L.A.); kuaanan.t@psu.ac.th (K.T.); mdshahariar.c@psu.ac.th (M.S.C.)
[2] Energy Technology Program, Department of Specialized Engineering, Faculty of Engineering, Prince of Songkla University, Hat Yai 90110, Thailand; arkom.p@psu.ac.th
[3] Department of Chemical Engineering, Balochistan University of Information Technology, Engineering and Management Sciences, Quetta 87300, Pakistan; asad.ullah1@buitms.edu.pk
* Correspondence: khamphe.p@psu.ac.th

Abstract: This study investigated the characteristics of biochars derived from the pyrolysis of rubberwood sawdust (RWS) and sewage sludge (SS) and their co-pyrolysis at mixing ratios of 50:50 and 75:25. Biochars were produced at 550 °C through slow pyrolysis in a moving bed reactor and then characterized. Results showed that the rubberwood sawdust biochar (RWSB) had high carbon content (86.70 wt%) and low oxygen content (7.89 wt%). By contrast, the sewage sludge biochar (SSB) had high ash content (65.61 wt%) and low carbon content (24.27 wt%). The blending of RWS with SS at the mentioned ratios helped enhance the gross and element contents of the biochar samples. The elemental analysis of the biochars was also reported in the form of atomic ratios (H/C and O/C). The functional groups of biochars were observed by Fourier-transform infrared spectroscopy (FTIR). X-ray fluorescence spectroscopy (XRF) revealed that the biochar from SS contained a high content of inorganic elements, such as Si, Ca, Fe, K, Mg, P, and Zn. The pH of the biochars ranged from 8.41 to 10.02. Brunauer, Emmett, and Teller (BET) and scanning electron microscopy (SEM) showed that RWSB had a lower surface area and larger pore diameter than the other biochars. The water holding capacity (WHC) and water releasing ability (WRA) of the biochars were in the range of 1.01–3.08 mL/g and 1.19–52.42 wt%, respectively. These results will be the guideline for further application and study of biochar from RWS, SS, and blended samples.

Keywords: biomass; biochar; bio-economy; biochar properties; organic wastes; soil improvement; bio-fertilizer

Citation: Ali, L.; Palamanit, A.; Techato, K.; Ullah, A.; Chowdhury, M.S.; Phoungthong, K. Characteristics of Biochars Derived from the Pyrolysis and Co-Pyrolysis of Rubberwood Sawdust and Sewage Sludge for Further Applications. *Sustainability* **2022**, *14*, 3829. https://doi.org/10.3390/su14073829

Academic Editor: Agostina Chiavola

Received: 6 February 2022
Accepted: 19 March 2022
Published: 24 March 2022

1. Introduction

The heavy utilization of natural resources, such as fossil fuels, water, and land, along with the rapid growth of population, leads to serious environmental problems [1]. Global warming and climate change cause variation in precipitation, flooding, high frequency of extreme weather, and low quality of agricultural soil [2,3]. The lack of water and land and the low quality of soil are serious agricultural problems. The rapid growth of population also increases the demand for vegetables and crops. These issues can be overcome through circular utilization or zero waste applications of natural resources. Conventionally, agricultural production requires plantation of crops. With this plantation, not only water and land or soils are important for growth; fertilizers are also necessary to increase product yield and increase the growth rate. However, the long-term utilization of land or soil leads to low-quality soil because of its lack of nutrients. The improvement of soil quality by using organic-based materials is gaining interest because this method is eco-friendly,

following the concept of bio-circular-green economy. When selecting fertilizers and soil improvement agents, farmers have many choices. These choices consist of organic and inorganic materials. Inorganic fertilizers take the form of ammonium nitrate, urea, rock phosphate, potassium chloride, and potassium sulfate [4]. Most utilized fertilizers are chemical products. Utilization of phosphate fertilizers affects ecosystems with eutrophication of water bodies and algal blooms [5,6]. In addition, the exploitation of fields can eventually deplete them of some essential nutrients, reducing crop yields in the future. Therefore, sustainable approaches that avoid chemical fertilizer use may be ecologically advantageous [7]. Biochar is considered a green material for removing hazardous elements, such as metals, metalloids, or non-metals, in groundwater and wastewater. This type of absorbent has a very low impact on ecosystems. It is also easy to apply, highly efficient, low cost, and widely available [8–10].

Biochar is the carbon dense material obtained from pyrolysis of biomasses or organic solid wastes, and is recently gaining more and more interest as a bio-fertilizer for soil and a mitigator of greenhouse emissions [11,12]. According to EBC [13], biochar is a heterogeneous substance rich in aromatic carbon and minerals. It is produced by pyrolysis of sustainably obtained biomass under controlled conditions with clean technology and is used for any purpose that does not involve its rapid mineralization to CO_2, and may eventually become a soil amendment. Pyrolysis is thermal decomposition of the feedstocks under absent oxygen or air atmosphere to produce the bio-oil, biochar and pyrolysis gas, depending on pyrolysis types. Slow pyrolysis is widely used to produce biochar with high product yield and quality. During this process, the physical and chemical properties of the feedstocks become a highly porous, stable, and carbon-rich material (biochar) with a vast surface area [14]. Biochar can be produced from various types of biomasses, such as agricultural residues and wastes (woods, sawdust, straws, and peels), industrial organic wastes, organic municipal solid wastes, and sewage sludge from wastewater treatment systems in allover the globs [15]. Miyaoka et al. [16] reported that the production of sewage sludge from wastewater treatment plants in Bangkok, Thailand, is 30,000–350,000 m3/day. However, Parkpian et al. [17] predicted that the Bangkok sewage sludge waste contained a large quantity of organic matter, as well as valuable nutrients like N, P and K, which are elements that can be reused in soil for increasing crop productivity as fertilizer after proper recycling process. Therefore, the Thai government should consider taking advantage of this cheap waste to potential bioenergy. SS obtained from agro-industries as a bio-waste can be applied as a product following the concept of circular bioeconomy. In degradation using thermal processes, it helps increase the value of low-grade biomasses and organic wastes [18,19]. Management and utilization of SS can be performed by open dumping, land filling, and converting it into new products. Turning the SS into biochar by pyrolysis is gaining attention because it helps eliminate or remove some undesired organic and inorganic components in SS such as antibiotics, pathogens, and heavy metals [20]. Previous studies have reported that the co-pyrolysis of biomass and SS improves the yield and quality of products [20,21]. They indicated that the properties of SS biochars (SSBs) depend on many factors, such type of SS, condition for producing biochar, and type of reactor [22]. The biochar obtained from some SSs has low carbon content with low porous structure and high heavy metal content [23]. According to Yang et al. [24], due to the rapid growth of industrialization and urbanization, a large quantity of heavy metals in the environments are creating more serious pollution in the form of various solid mediums. Consequently, the properties of biochar production from SS can be improved by mixing with other types of feedstocks. For example, coal or biomass has been mixed with sewage sludges and with paper waste for pyrolysis or co-pyrolysis [25,26]. Thus, biochar produced at high pyrolysis temperature increases persistence due to resistance to microbial and chemical decomposition in soil [27]. By contrast, low temperature (<400 °C) biochar has high yield, low pH, and contains several essential nutrients and easily decomposable substrates [28]. Pyrolysis of mixed biomasses or feedstocks is called co-pyrolysis. This process both enhances product yield and improves product properties. Ali et al. [25,26] and Sakulkit et al. [29]

explored the pyrolysis and co-pyrolysis of feedstocks and they found that product yield and characteristics are strongly dependent on the type of reactor and operating conditions. This finding indicates that pyrolysis and co-pyrolysis of feedstocks at elevated temperature under inert atmosphere for producing bio-oil, pyrolysis gas, or biochar needs to perform at appropriate condition [30]. Thus, solid by-products such as biochar (bio-fertilizer) of pyrolysis can be applied in places with supporting economy and zero investments.

Remesh [31] predicted that the use of organic manures, particularly bio-fertilizers, is the only sustain way to improve the soil organic carbon for sustenance of soil quality and future productivity. The biochar can be used as a bio-fertilizer because of its high concentration of nutrients, especially potassium (K) and phosphorus (P) [32]. Moreover, Dai et al. [33] and Novotny et al. [34] reported that the C, N, K, Mg, Ca, and P nutrient concentration may be advantageous when they enter in soil for crops growth with together of biochar. The physicochemical characteristics of biochar, such as polarity, surface area, atomic ratio, elemental composition, and porosity, can be affected by those choices [35]. The application of biochar is not limited to remediation of polluted soil. It can also increase crop yield and improve healthy soil properties. According to the Sustainable Development Goals (SDGs-6), biochar is the best option for cleaning water and adsorbing soil pollutants [36]. It can also be applied in cosmetics and in removing dyes from sensitive surfaces and leachates from soil [37].

For soil fertility, biochar can play a key role as a soil conditioner because of its high carbon content, and it can improve the physicochemical and biological properties of soil. Organic carbon is an organic fertilizer that can increase the water retention capacity of soil [38]. Moreover, the WHC of soil depends on the specific surface of biochar and its hydrophobicity [39]. Notably, the biochars produced for the current study were derived from the slow pyrolysis of RWS biomass and SS organic waste feedstocks with different blended ratios (50:50, 75:25) and decomposed by pyrolysis and co-pyrolysis. Biochar derived from RWS was more suitable for soil amendment than biochar derived SS because of its contained (RWSB), a higher pore volume, lower number of heavy metals, and lower ash content it can be better alternative to use as bio-sorbent and bio-fertilizer in land for crops growth. Moreover, a high fixed carbon content and low ash content with high porosity make biochar a competitive candidate as a bio-filter for wastewater treatment as well as for solid fuel [40]. In the case of SS biochar, it is a mixture of organic matters. It contains a higher number of noxious elements, including Cd and Pb, which are not acceptable for use as soil as conditioners or filtration but can be used as solid fuel due to its higher ash content [40]. In contrast, according to EBC [13] guidelines for biochar application, the SSB of this study were not appropriate for use as soil amendment because the heavy metal content, especially Cd and Pb, was too high. Thus, management of such types of cheap residues and waste of local materials to convert into green biochar can improve agronomic and environmental performance in soil [15]. The scientific contribution of this research is to evaluate the use of local waste materials as a new raw material to produce biochar, which can further serve as a sustainable remediation for soil and solid fuel source. This study explores the characteristics of biochar obtained from the pyrolysis of lignocellulosic biomass (RWS) and sewage sludge (SS) and biochar from the co-pyrolysis of these feedstocks at mixing ratios of 50:50 and 75:25 (RWS:SS). The bulk density, proximate and ultimate characteristics, atomic ratios, TGA characteristics, pH, CS, SEM characteristics, BET characteristics, FTIR spectra, WHC, and WRA of the biochar samples are investigated.

2. Materials and Methods

2.1. Biochar Preparation

RWS was collected from a rubberwood factory in Khlong Ngae, Sadao District, Songkhla Province, Thailand. SS was obtained from canned tuna factory located in Hat Yai city, Songkhla Province, Thailand. For co-pyrolysis, the ground RWS and SS samples were mixed thoroughly at different ratios to RWS50:SS50 and RWS75:SS25 (wt%). Furthermore, pyrolysis and co-pyrolysis of RWS and SS biomass feedstocks were carried out by slow

pyrolysis with a cylindrical-shaped moving bed pyrolysis reactor. The reactor was preheated to the set pyrolysis temperature of 550 °C with a heating rate of 10 °C/min under a nitrogen (N_2) gas atmosphere for 45 min, and the feedstocks were converted into biochar at this temperature. After processing, the biochars were stored in containers to cool down and then placed in desiccators to prevent absorption of moisture. The prepared biochars were either used in this state or tested further.

2.2. Biochar Properties

The physical and chemical properties of the prepared biochars (RWS, SS, RWS50:SS50, and RWS75:SS25) were studied as described below. All experiments were carried out in triplicate.

2.3. Determination of Biochar Characteristics

2.3.1. Basic Components and Atomic Ratios

The biochar samples were characterized using proximate analysis, ultimate analysis, X-ray fluorescence spectroscopy (XRF), thermogravimetric analysis (TGA), pH, carbon sequestration (CS), scanning electron microscope (SEM), Brunauer–Emmett–Teller (BET), Fourier transform infrared (FTIR), water holding capacity (WHC), water releasing ability (WRA), and H/C and O/C atomic ratios. The ultimate analysis of CHNOS on a dry basis was performed on a Thermo Scientific FLASH 2000 Organic Elemental Analyzer (Thermo Scientific, Milan, Italy) with an in-house method, whereas the oxygen (O) of biochar was calculated as the difference from other ultimate analysis values ($O = 100 - C - H - N - S - Ash$) [41]. The proximate analysis was done on an as-received basis and was conducted using macro-TGA (TGA 701, LECO, St. Joseph, MI, USA) in accordance with ASTM D7582. The H/C and O/C atomic ratios (on a dry basis) in the biochars were determined via the Van Krevelen method and were compared with those reported in previous studies [42].

2.3.2. Major and Minor Elements

The major and minor elements reported for the biochars include Si, Ca, Fe, K, Mg, Na, P, Cu, Zn, Mn, Cd, and Pb. The biochars were subjected to XRF spectrometry (Zetium, PANalytical, Almelo, The Netherlands).

2.3.3. Thermogravimetric Analysis

The thermal decomposition of the biochars RWS, SS, RWS50:SS50, and RWS75:SS25 was analyzed using TGA and differential thermal analysis in a thermogravimetric analyzer (Perkin Emer, USA) in accordance with ASTM E1131. The equipment was heated with N_2 atmosphere from room temperature to 50 °C–1000 °C at a rate of 10 °C/min. A sample of approximately 3 g was used in each run.

2.3.4. pH of Biochar

The pH of biochar samples was measured (UB-10 Denver Instrument) at room temperature. The 1 g biochar sample was mixed with 20 mL of deionized water in a 50 mL glass bottle for 30 min on a shaker. The pH meter was calibrated with pH 4, pH 7, and pH 10 buffers before use. All cases were measured in triplicates [43].

2.3.5. Carbon Sequestration (CS)

The CS index R50 was applied to assess the thermal recalcitrance of the freshly produced biochars. The thermal recalcitrance of biochar can be acquired from TGA as previously described by Harvey et al. [44]:

$$R_{50,biochar} = \frac{T_{50,biochar}}{T_{50,graphite}}, \quad (1)$$

where $T_{50,\ biochar}$ and $T_{50,\ graphite}$ are different temperatures at which 50% weight loss was caused by oxidation and volatilization of biochar and graphite, respectively. The water and ash contents were subtracted from the TG thermograms, and the temperature was obtained directly. Thus, the last retained carbon in the solid is known as CS potential. It is calculated by subtracting the carbon loss during pyrolysis from the initial C in raw biomass and multiplying by the recalcitrance (R_{50}) of C in the biochar [45] as follows:

$$\text{Carbon sequestration } (\%) = \frac{M_{(g)} \times \text{Yield } (\%) \times C\%_{\text{Biochar}} \times R_{50}}{M_{(g)} \times C\%_{\text{Feedstock}}}, \quad (2)$$

where

M = Weight of the total feedstock (g)
Yield = Pyrolyzed biochar amount (%wt.)
C Biochar = Carbon amount of biochar (%)
C Feedstock = Carbon amount of feedstock (%)

2.3.6. SEM and BET Analysis

SEM of the biochars was performed under high vacuum conditions with an accelerating voltage of 20 kV (JSM-5800 LV, JEOL, Tokyo, Japan), and a secondary electron (SE2) detector with a magnification of 500X [46]. Prior to observation, each sample was sputter coated with gold. The surface area of the biochar sample was determined by the Brunauer–Emmett–Teller (BET) method (ASAP2460, Micromeritics, Norcross, GA, USA) and the static volumetric N_2 gas adsorption method. The sample was pretreated under vacuum condition at temperature of 80–200 °C for 15 h. The adsorption–desorption isotherm was determined by the static volumetric method. The N_2 gas was used as carrier gas and adsorbed gas. The pore volume was obtained from the adsorption isotherm with the multi condensation point (p/p0 = 0.05–0.03, 10–20 points). The pore structure was determined from the adsorption isotherm and the average width was calculated by using the formula 4 V/A (V represents the pore volume while A denotes the adsorbed bet specific surface area) [46].

2.3.7. Functional Groups

The active organic functional groups of the biochars were identified via FTIR spectroscopy. The biochar from pyrolysis or co-pyrolysis at 550 °C was subjected to FTIR (Vertex70, Bruker, Ettlingen, Germany). Each spectrum was an average of 32 scans from 400–4000 cm^{-1} at 4 cm^{-1} spectral resolution. The FTIR results were elucidated based on a literary survey.

2.4. Hydraulic Properties of Biochar

The main hydraulic properties, including WHC and WRA, of the biochars were determined. WHC was determined using an in-house method. Before the experiment, the glass beakers and filter papers were oven dried. The biochar samples were also heated in an oven for 10 h at 105 °C (or until reaching a constant mass). The dry biochar samples were soaked in deionized water for complete saturation in a cylindrical glass beaker for 24 h [47]. Then, the excess water on the biochar surface was drained over 30 min. During draining, dry filter papers were used to hold the biochars, and then the moist biochar samples were weighed using a digital balance. Meanwhile, wet filter papers with particles were placed in an oven for drying. The filter papers were dried again and then weighed, and the remaining particle weight from the total biochar sample on the filter paper was determined. Thus, the water free biochar samples and the water retained in the samples were determined by weight for a comparison of before and after [48]. The WHC was calculated as follows:

$$\text{WHC } (mL/g) = \frac{\text{water retained biochar } - \text{ dry biochar}}{\text{dry biochar}} \quad (3)$$

The WRA of the biochar samples was determined using an in-house method at an ambient room temperature of 25 °C. After removing surface water on biochar, the moist biochar was stored at room temperature for air drying naturally. The samples were stored for 12 h and then weighed every hour. After sufficient drying time, the biochar samples were weighed. The mass of water released (WRAS) and the mass of water remaining (WRAM) of the biochars were estimated as follows:

$$\text{Water releasing ability (WRA\%)} = \frac{(\text{Xi} - \text{Xit})}{\text{Xit}} \times 100, \quad (4)$$

$$\text{Water remaining ability (WRA\%)} = 100 - \text{WRA}, \quad (5)$$

where

At t = 0, Xi = Xit, WRAS0 = 100%
Xi = Mean mass of water before releasing at each period
Xit = Mean mass of water after releasing at the final period
t = time

3. Results and Discussion

3.1. Characterization of Biochar

3.1.1. Proximate Analysis and Bulk Density

The proximate analysis and bulk density of the biochars from RWS, SS, RWS50:SS50, and RWS75:SS25 are shown in Table 1. Proximate analysis and bulk density were significantly higher, and differences among these samples were determined using one-way ANOVA. The moisture content, volatile matter, fixed carbon, and ash content were 4.44–4.95, 11.51–14.40, 15.04–78.26, and 5.79–65.61 wt%, respectively. The results were directly correlated with feedstock types, whereas pyrolysis or co-pyrolysis temperatures could also have been manipulated. The moisture content retained in the biochar was not zero even when pyrolyzed at a high temperature, which agrees with previous studies by Kabir et al. [49] and Palamanit et al. [46]. Both of these prior studies reported moisture contents in the range of 2.40–4.42 (wt%). However, the moisture content affected biochar yield. A high moisture in the biomass was favorable for the biochar yield from processing at a high pressure [50]. The volatile matter, including the comparatively light-molecular-weight components in liquid or gas form, in the biochars reduced as the temperature was increased [46]. The volatile matter in biochar remained in the range of 4.32–14.40 wt%, indicating that the pyrolysis was incomplete while full decomposition would need more time or higher temperatures. Escape of volatile matter from the pores of biochar during production enhanced soil water movement and soil water retention characteristics [51]. Moreover, the high fixed carbon content in biochar indicated a loss of volatile matter from the biochar. Palamanit et al. [46] and Bhattacharjee and Biswas [52] reported that a high amount of fixed carbon in biochar is favorable for use as a solid fuel because of high energy content. The fixed carbon is helpful in improving biochar stability during carbon storage. The ash content of SSB was higher than that in RWSB and in the blends. According to Dume et al. [53], if the ash content of biochar is higher than 35% then the fixed carbon will be lower than 30%; they are inverse to each other. Nevertheless, the ash contents in both raw biomasses and biochars are common and constitute non-volatile and non-combustible components. In the case of soil improvement, the biochar produced in this study from slow pyrolysis is more feasible for healthy biochar than fast pyrolysis. Comparing the fast and slow pyrolysis produced biochars, the slow pyrolysis biochars often demonstrated higher porosity, content of nutrients, and organic substrates, and had greater ability to mitigate N_2O emissions from soils [54].

Table 1. Proximate analysis, ultimate analysis, bulk density, and atomic ratios of biochar samples.

Property	Biochar Samples					
	RWS	SS	RWS50:SS50	RWS75:SS25	PPS500 [1]	OPT [2]
Proximate analysis (wt%, as-received basis)						
Moisture content (MC)	4.44 ± 0.03 [a]	4.95 ± 0.07 [d]	4.71 ± 0.01 [c]	4.55 ± 0.03 [b]	6.09	3.27
Volatile matter (VM)	11.51 ± 0.01 [a]	14.40 ± 0.01 [d]	12.95 ± 0.00 [b]	12.54 ± 0.08 [b]	4.32	14.15
Fixed carbon (FC)	78.26 ± 0.01 [d]	15.04 ± 0.02 [a]	46.63 ± 0.02 [b]	62.42 ± 0.02 [c]	85.36	74.26
Ash content (AC)	5.79 ± 0.02 [a]	65.61 ± 0.02 [d]	35.71 ± 0.01 [c]	20.49 ± 0.00 [b]	54.77	8.32
Ultimate analysis (wt%, as-dry basis)						
Carbon (C)	86.70 ± 0.10 [d]	24.27 ± 0.03 [a]	55.14 ± 0.00 [b]	71.15 ± 0.13 [c]	80.79	77.45
Hydrogen (H)	3.32 ± 0.40 [d]	0.87 ± 0.01 [a]	2.10 ± 0.00 [b]	2.73 ± 0.05 [c]	3.29	2.38
Nitrogen (N)	0.49 ± 0.00 [a]	2.97 ± 0.03 [d]	1.73 ± 0.01 [c]	1.10 ± 0.00 [b]	0.27	0.51
Sulfur (S)	0.04 ± 0.00 [a]	0.44 ± 0.01 [d]	0.25 ± 0.01 [c]	0.10 ± 0.01 [b]	N/A	0.06
Oxygen (O)	7.89 ± 0.60 [d]	5.13 ± 0.07 [a]	6.11 ± 0.05 [b]	6.65 ± 0.09 [c]	11.13	11
Bulk density (kg/m^3)	181.74 ± 0.45 [a]	567.32 ± 0.58 [d]	317.87 ± 0.4 [c]	273.86 ± 0.49 [b]	225	N/A
H/C	0.46 [b]	0.43 [a]	0.45 [a]	0.46 [b]	0.04	0.43
O/C	0.07 [a]	0.16 [b]	0.08 [a]	0.07 [a]	0.14	0.43

PPS500 and OPT mean pigeon pea stalk and oil palm trunk, respectively. [1,2] Results from Sahoo et al. [55] and Sakulkit et al. [29]. N/A means not available. Data represent the averages and standard deviations based on triplicate experiments. Comparisons between the 12 treatments are significantly different (Tukey, $p < 0.05$), and each treatment is indicated by lowercase letters (a–d).

The bulk densities of the RWS, SS, RWS50:SS50, and RWS75:SS25 biochars were in the range of 181.74–567.32 (kg/m^3), as shown in Table 1. RWSB had a lower bulk density than SSB or blends of RWSB with SSB because SSB had a much higher ash content of metallic elements than the other samples. Moreover, the bulk density of the biochar samples is dependent on biomass feedstock type. Bulk density is important to the potential applications because low-density biochars need a large area or volume for storage and transportation [46]. Conversely, a low bulk density is caused by high porosity, which affects the potential for soil aeration and enhances interactions with water [56].

3.1.2. Ultimate Analysis and Atomic Ratios of Biochar

Table 1 presents the elemental compositions and atomic ratios H/C and O/C of the RWS, SS, RWS50:SS50, and RWS75:SS25 biochars. The reported results from the ultimate analysis of biochars indicated that the atomic ratios of H/C and O/C were similar. The one-way ANOVA tests produced results higher than those obtained using other methods. The carbon, hydrogen, nitrogen, sulfur, and oxygen contents of the biochars were in the ranges of 24.27–86.70, 0.87–3.32, 0.49–2.97, 0.04–0.44, and 5.13–7.89 wt%, respectively. The ultimate analyses were consistent with the proximate analyses, as indicated by the relation between volatile matter and fixed carbon content and hydrogen and nitrogen contents. The carbon contents in SSB and its blends with RWSB were below those in RWSB alone. The thermal decomposition temperatures were affected by biochar structure and composition. The results clearly show that the biochars from pyrolysis have increased carbon and reduced oxygen contents, which is a similar result to those of recent studies [29,55,57]. Several studies have reported that carbon-rich biochar has good potential for soil amendment. In addition, it stabilizes or immobilizes heavy metals in the soil and decreases concentrations of hazardous metals in plants. In other words, the biochar with a higher C content can be used as bio-catalysts in microbial fuel cell (MFC) technology to produce electricity after modification [58]. In this study, the RWSB had a higher C and lower O; it was suitable to apply on soil for its improvements according to the above studies, and it may also be used in MFC. In contrast, the SSB had a very lower C and may be used for solid fuel. However, such performance depends on the types of feedstock and the experimental conditions [59,60]. Furthermore, the carbon in biochar is the key element in all the functional groups. Conversely, oxygen and hydrogen contents of biomass feedstock

strongly influence biochar properties, including association, disassociation, and polarity of hydrogen ions, which can strongly impact the biochar interactions with organic and inorganic solutes [61].

The H/C and O/C ratios in the biochar samples were in the ranges of 0.43–0.46 and 0.07–0.16, respectively. The H/C and O/C atomic ratios decreased as the temperature of carbonization increased; Table 1 indicates they were stable in this study. These results are similar to those obtained by Wani et al. [62] and Sakulkit et al. [29]. Usevičiūtė and Baltrėnaitė-Gedienė [63] found that the H/C and O/C atomic ratios decrease with increasing temperature from 300 °C to 500 °C in pyrolysis of biomass (grass and wood). Normally, demethylation (CH_3) is evaluated from the H/C ratio, whereas decarboxylation (CO_2) is assessed from the O/C ratio, and the eventual solid biochar is enriched in carbon content [64]. The main purpose of evaluating the H/C and O/C atomic ratios is for use as proxy indicators of biochar stability, and these correlate negatively with aromatic carbon. However, biochar produced at a comparatively low temperature with a high O/C ratio can have low carbonization and lacks stability against degradation in the soil surface. Thus, it displays comparatively high reactivity [48,63]. According to the European Biochar Foundation (EBC), biochar H/C ratio must be below 0.6 while O/C must be below 0.4 in carbon black substances [65]. In the present study, the H/C and O/C atomic ratios satisfy these criteria, and the biochars are therefore suitable for further soil application.

3.1.3. X-ray Fluorescence (XRF)

Table 2 presents the major and minor inorganic elements in the RWS, SS, RWS50:SS50, and RWS75:SS25 biochars, as identified by XRF spectrometry. The inorganic elements in the biochars were Si (6731–102,415.3), Ca (116,085.7–241,156.7), Fe (1308–104,031.3), K (23,540–49,341.33), Mg (7283.33–14,071.67), Na (291–7818), P (3120–183,740), Cu (110–1120), Zn (130–11,660), Mn (750–6170), and Pb (32.98–131), (mg/kg). The concentrations of Si, Al, and Ca were higher in SSB than in RWSB or in their blend ratios (50:50 and 75:25). RWSB had less Na than the other biochars. Pb was detected only in SSB or the blends but not in RWSB. When a large portion of SS waste was co-pyrolyzed with RWS, the inorganics in the biochars decreased. Furthermore, the major and minor inorganic elements identified in the biomass and in the pyrolyzed biochar originated from the plant biomass. That is, they are present in the plants naturally [66]. The results of this current study are similar to those obtained by Deng et al. [67] and Kończak et al. [68]. According to Deng et al. [67], K, Ca, Mg, Na, Si, Fe, and Al are the dominant elements in SS waste char from pyrolysis or co-pyrolysis. Previous studies reported that the inorganic elements are often retained in SSB after pyrolysis because they do not decompose or become volatile at pyrolysis temperatures of 400–600 °C [69–71]. The application of biochar with appropriate elements for soil improvement can increase crop productivity by reducing toxic elements via electrostatic reactions [72]. Notably, biochar has many major and minor inorganic elements that are essential for crop growth and soil health. According to EBC guidelines, if the Pb, Ni, Cr, Cd, Cu, and Zn concentrations in biochar do not exceed the limit values [65], such biochar could be recommended for incorporation into the soil. Therefore, Ca, K, P, and Mg were found in SSB and RWSB in this study, but some elements such as Cd and Pb are unacceptable for soil application because they exceeded recommended limits. Therefore, the biochar from RWS blended with SS may be useful for soil remediation and positively influencing crops because of the balance in inorganic element concentrations [25].

Table 2. Major and minor elements of biochar samples.

Elements (mg/kg)	Biochar Samples					
	RWS	**SS**	**RWS50:SS50**	**RWS75:SS25**	**SC550-30** [1]	**CMB600** [2]
Silicon (Si)	6731	102,415.3	54,572.82	7552.41	14,100	30,000
Calcium (Ca)	241,156.7	116,085.7	178,621.2	209,889.3	140,700	62,000
Iron (Fe)	1308	104,031.3	52,669.1	26,988.5	287,500	N/A
Potassium (K)	23,540	49,341.33	36,441	29,982.4	2500	380,000
Magnesium (Mg)	7283.33	14,071.67	10,677.54	8980.76	2700	9000
Sodium (Na)	291	7818	4055.57	2172.11	9500	81,000
Phosphorus (P)	3120	183,740	122,720	71,640	73,600	53,000
Copper (Cu)	110	1120	830	560	N/A	N/A
Zinc (Zn)	130	11,660	7780	4530	N/A	N/A
Manganese (Mn)	750	6170	4400	2880	1400	N/A
Lead (Pb)	ND	131	65.57	32.98	N/A	N/A
Cadmium (Cd)	ND	ND	ND	ND	ND	ND

In this study, ND and N/A mean not detected and not available, respectively; SC550-30 (SC550-30 = TDS: RWW), and CMB600 mean textile dyeing sludge: red wood waste and chicken manure biochar. [1,2] Results from Zhou et al. [73], and Huang et al. [74], respectively.

3.1.4. Thermogravimetric Analysis

Figure 1a,b show the TGA curves with peaks, with TGA in (wt%) and DTG also in (wt%), for RWSB and SSB. TGA and DTG were performed to evaluate the pyrolytic behavior and biochar resistance to thermal decomposition [10]. As shown in Figure 1a,b, thermal decomposition of biochars at temperatures of 50–1000 °C was low. At a temperature range of 50–250 °C, the thermal decomposition trend of each biochar was similar. The weight loss in this stage was due to the elimination of water or moisture, which was consistent with the moisture content from the proximate analysis. With higher temperatures, the thermal decomposition trend of RWSB was prominent compared to other samples. The weight of RWSB was slowly reduced at temperatures between 250 °C to 700 °C. In DTG, the highest peak for RWSB was noted at approximately 700 °C because of the remaining lignin fraction. In the present study, the feedstocks were produced as biochar at 550 °C for further characterization. Thus, the lignin did not decompose completely at this point, whereas the SSB at this temperature was mostly stable. This is due to the main component of biochar from SS being ash, as observed from the proximate analysis results. The obtained results were similar to the study of Hamza et al. [75]. They reported that the TGA and DTG curves in their biochars flatten at high temperatures approximately above 610 °C because of the aromatization of the lignin part, preventing the loss of additional weight. Moreover, the degradation rates of RWSB and SSB were similar to those in Kim et al. [76] and Reza et al. [10]. Remarkably, the weight loss at higher temperatures was attributed to the degradation of inorganic compounds and the dehydrogenation and aromatization of biochar [77]. A comparatively low weight loss is suitable for a stable biochar with strong carbon–carbon and hydrogen–carbon bonds remaining [78].

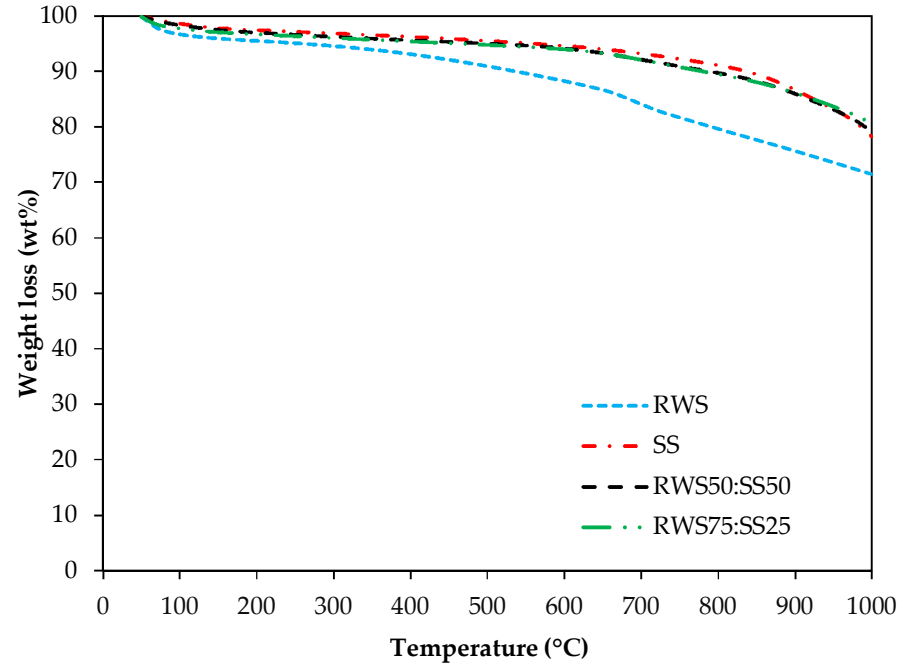

(**a**)

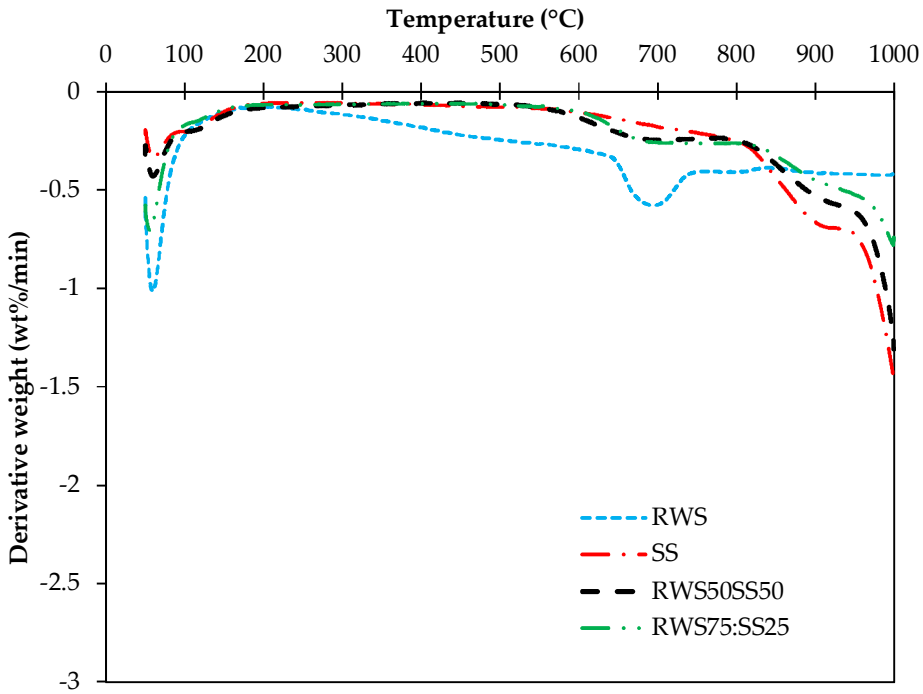

(**b**)

Figure 1. TGA (**a**), and DTG (**b**) of RWS, SS, RWS50:SS50 and RWS75:SS25 biochars from pyrolysis at 550 °C.

3.1.5. pH Analysis

Figure 2 shows the pH values of the RWS, SS, RWS50:SS50, and RWS75:SS25 biochars were in range of 10.02, 8.41, 8.69, and 9.04 from pyrolysis at 550 °C, respectively. The pH results of the biochars samples were compared, and results showed significant differences among the samples when analyzed by one-way ANOVA. RWSB had much higher pH (was more strongly alkaline) than SSB or their blends. The lower pH of SSB might be from the

acidity of organic oily components. Normally, pH increases with pyrolysis temperature of biochar [79]. Moreover, biochar pH increases because of elimination of organic materials while the alkaline salts are retained [80]. However, the biochar surface functional groups, such as phenolic, carboxylic, and lactonic groups, could be associated with biochar sorption capacity [48]. The pH levels of RWSB and SSB in this study are similar to those obtained in previous studies by Angın [81], Ferreira et al. [82], and Reza et al. [10]. Conversely, Han et al. [83] reported that the low pH of biochar can be relatively influenced because the hydrogen H^+ ions engage the biochar adsorption pour sites. Biochar with high pH has more potential for use as a soil conditioner that reduces heavy metal contaminants. In addition, biochar with suitable pH can enhance the aeration, moisture, and redox potential of weaker soil surface by reducing the pollutants [8]. Duku et al. [84] described that biochar with high pH is advantageous for soil health and can limit the need to use lime in soils. It can also develop the loamy and sandy properties in soils effectively against clay soils; this has been successfully achieved in Pennsylvania, Ghana, and Mexico. The RWSB pH has potential for agriculture use, according to Duku et al. [84]. Therefore, the biochar from pyrolysis at an intermediate temperature has great potential for soil use as organic carbon due to its good water capacity and exchangeable cation content, and it may decrease the ductile strength of soil surface [85].

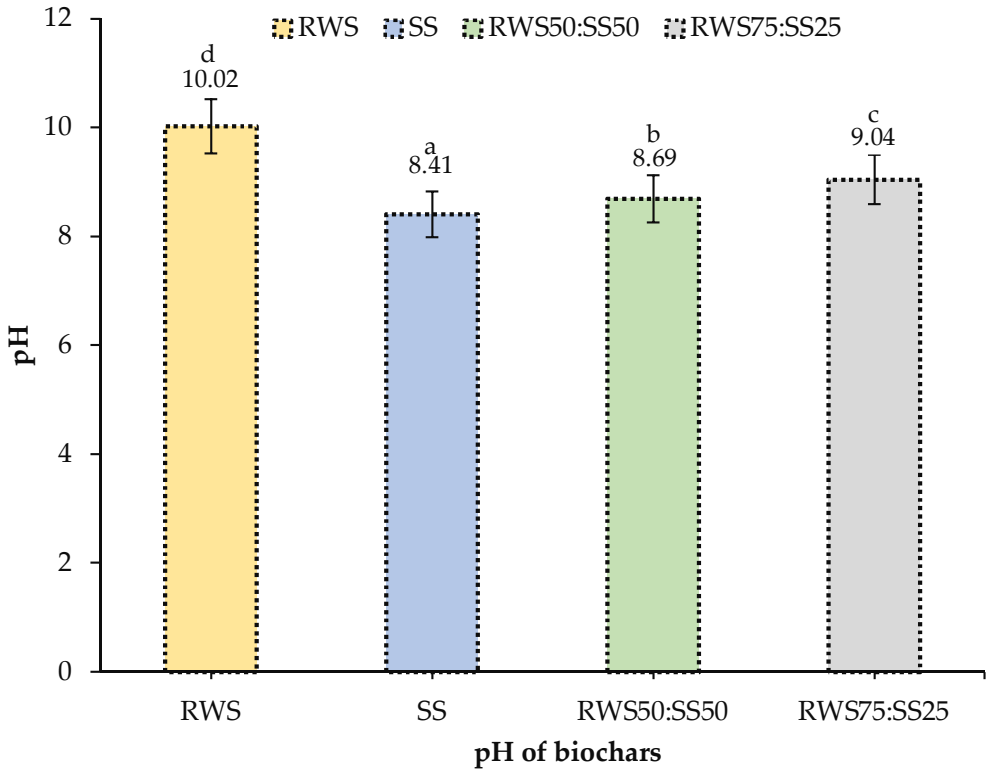

Figure 2. pH levels of RWS, SS, RWS50:SS50, and RWS75:SS25 biochars from pyrolysis at 550 °C. Data represent the averages and standard deviations based on triplicate experiments. Comparisons among the four treatments were significantly different (Tukey, $p < 0.05$) and all the treatments are indicated by lowercase letters (a–d).

3.1.6. Recalcitrance and Stability of Biochars

Table 3 shows the CS and recalcitrance of RWSB, SSB, and their blends (50:50 and 75:25). The calculated R_{50} and CS for biochar samples were in the ranges 0.28–0.54 and 11.03–22.73 (%), respectively. The index (R_{50}) for carbonized biochar is based on a model proposed by Harvey et al. [44]. For soil maintenance functionality and stability, as related to atmospheric CS, biochar materials need to resist biotic or abiotic degradation. The R_{50} index is a measure of the energy required for thermal oxidation at 50% weight loss of biochar.

The temperatures determined for R_{50} were obtained from thermograms corrected for ash and water contents, and were found to be in the range of 450–492 °C. It can be seen that the obtained results of this study are similar to Shrivastava et al. [57]. The pyrolysis temperature can influence the biochar recalcitrance, which is connected to aromatic C. Further, with increasing pyrolysis temperature, causing loss of N, aromatic C can increase [86]. However, the reacting temperatures have a dominating capability to control of the recalcitrance of the biochar nature. Moreover, for CS, the R_{50} index is combined with carbon contents from ultimate analysis and proximate analysis. A low pyrolysis temperature tends to create biochar with high carbon yields but with small pores and no resistance to abiotic or microbial mineralization. A higher pyrolysis temperature provides less biochar, but it is more stable and recalcitrant [87,88]. The biochar CS capability for $R_{50} > 0.7$ is comparable to soot or graphite [44].

Table 3. Recalcitrant nature of biochar samples.

Type of Biomass	Pyrolysis Temperature °C	Carbon Sequestration (%)			
		Carbon (wt%)	Fixed Carbon (wt%)	R_{50}	CS (%)
RWS	550	86.7	78.26	0.54	22.73
SS	550	24.27	15.04	0.28	11.03
RWS50:SS50	550	55.14	46.63	0.39	16.91
RWS75:SS25	550	71.15	62.42	0.48	19.89

3.1.7. Surface Morphology and Surface Area

Figure 3a–d present the SEM micrographs of RWS, SS, RWS50:SS50, and RWS75:SS25 biochars obtained from pyrolysis at 550 °C. The SEM images of biochar samples from RWSB and SSB and their blends show different surface features. In Figure 3a,b, it can be seen that RWSB and SSB were pyrolyzed singly, while Figure 3c,d shows blends. It can be observed that RWSB was rougher than SSB at SEM magnification 500X. The RWSB shows some cylindrical and honeycomb shapes. From woody biomass after pyrolysis at a higher temperature, the biochars appear more porous because of thermal degradation of lignocellulosic components. The RWSB surface features in this study are comparable to those in Palamanit et al. [46] and Sakulkit et al. [29]. As shown in Figure 3b, the SSB pores and features are not particularly clear because of their small particles and sandy characteristics. Hence, the SSB after pyrolysis did not have structural pores, as shown in Figure 3b. However, the co-pyrolysis of RWS biomass with SS at various blend ratios gave more porosity than SS for biochars, as seen in Figure 3c,d. Several factors affect the biochar produced, including residence time, temperature, and pyrolysis reactor type. [89]. Therefore, the decomposition of SS biomass alone at a higher temperature gave undeveloped pore structure biochar compared to RWSB because of the lower content of carbon in SS [90]. Biochar with high porosity can be applied as an adsorbent of heavy metals from the soil because the active sites on biochar can attract and reduce the toxic elements [91]. Biochar can also be used in microbial fuel cell (MFC) technology due to its biocompatibility, adequate resistance to corrosion, low ohmic resistance, high electrical conductivity, and low cost [58].

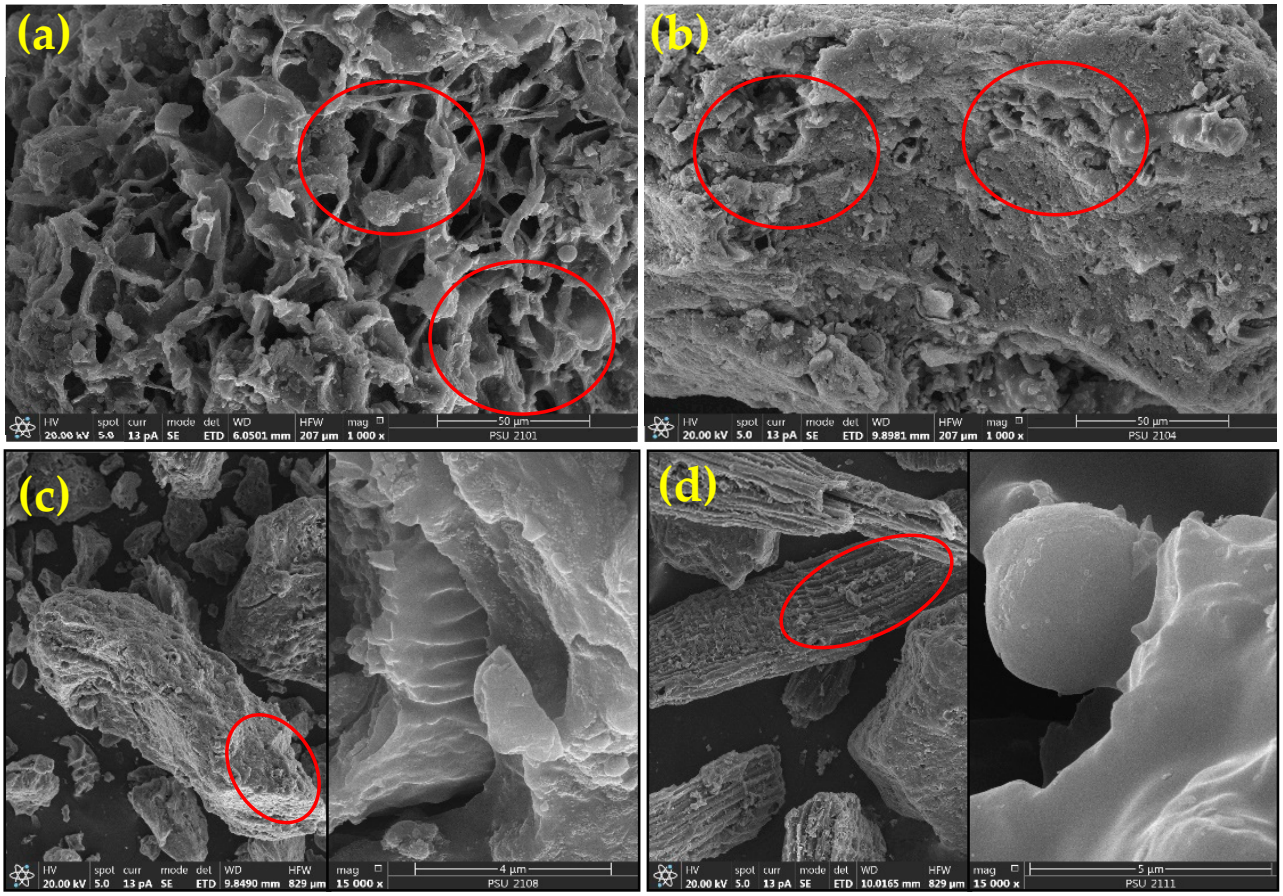

Figure 3. SEM photographs of (**a**) RWS biochar, (**b**) SS biochar, (**c**) RWS50:SS50 biochar, and (**d**) RWS75:SS25 biochar, (the right-side figures (**c**,**d**) show RWS biochar, while the left side shows SS biochar), and red circles show the pores of particles.

The surface area and average pore diameter of RWSB and SSB were found to be significantly higher using one-way ANOVA and BET, when each biomass feedstock was pyrolyzed at higher temperatures, as shown in Figure 4. The surface area and average pore diameter of biochar samples were in the ranges of 2.15–18.42 (m^2/g) and 162.39–217.16 (nm), respectively. The pore volume and pore diameter of SSB were lower than for RWSB or the blends. The specific surface area of RWSB was higher than for SSB, as seen in Figure 4. The surface area and pore volume of RWSB in this study were most similar to those obtained by Sakulkit et al. [29] and Shrivastava et al. [57]. Regarding SSB, prior studies include Agrafioti et al. [92] and Deng et al. [67]. Deng et al. [67] reported that the surface area of sewage sludge biochar was 27.9 (m^2/g), while Agrafioti et al. [92] found that it was 18 (m^2/g). However, co-pyrolysis of RWS mixed with SS biomass blended ratios from higher side biochar strongly influenced the lower side biochar, which affected the pore volume and surface area. The fact that RWS is a more lignocellulosic biomass also influenced these factors. The application of higher porous biochar with rich carbon content (SBET >100 m^2/g) could be used to develop the soil porosity by 2–40% and to reduce the soil higher bulk density by 3–30%, as theorized by Fidel et al. [93] and Mukherjee et al. [94].

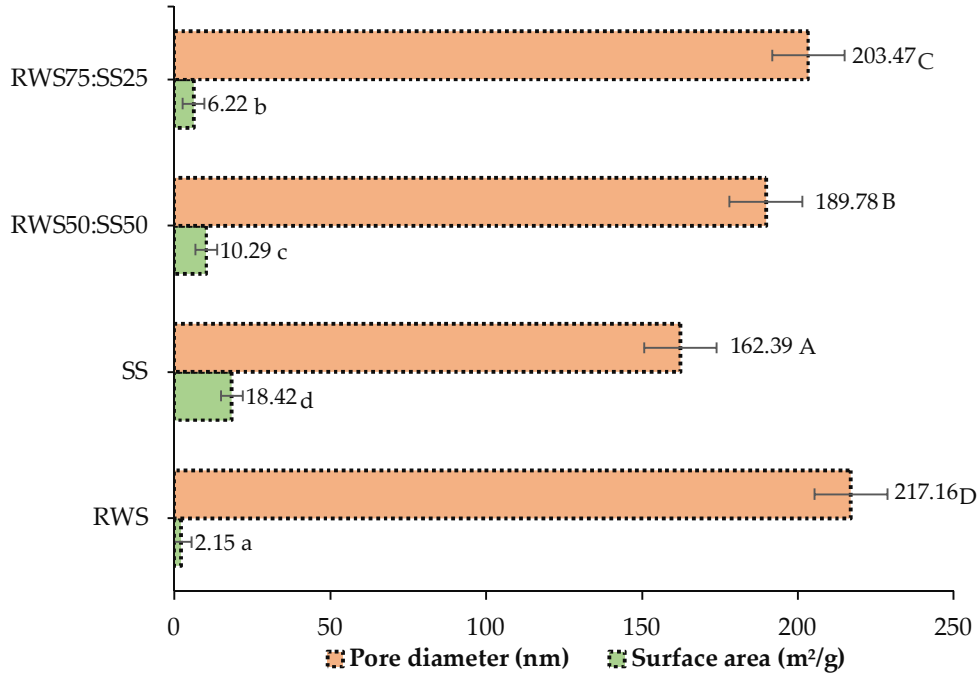

Figure 4. Specific surface area and pore diameter of RWS, SS, RWS50:SS50, and RWS75:SS25 biochars samples pyrolyzed at 550. Data represent the averages and standard deviations based on triplicate experiments. Comparisons among the eight treatments were significantly different (Tukey, $p < 0.05$). Pore diameters where treatments are indicated by capital letters (A–D) and surface areas are indicated by lowercase letters (a–d) are different.

3.1.8. FTIR Analysis Results

Figure 5 shows the FTIR results for RWSB, SSB, and their blends (50:50 and 75:25) from pyrolysis at 550 °C. Several components were present in the biochar samples, as shown in Figure 5. The biochar samples still contained compounds with C, H, and O despite strong degradation of the lignin component. The FTIR results correlate with ultimate and proximate analyses that were discussed in earlier sections. In addition, the biochar spectra did not differ significantly from each other because of similar C, H, and O contents. The first peak at approximately 3404–3410 cm^{-1} was attributed to OH group stretching and was associated with biomass dehydration due to phenols, alcohols, and carboxylic acids [95,96]. The second small peak at 2851–2873 cm^{-1} corresponded to C–H stretching vibrations in aliphatic and aromatics structures. The peak at 1605 cm^{-1} was for carbonyl and carboxyl groups in carbohydrates, ketones, and aldehydes, likely with a small quantity of amides [97]. The aromatic ring stretching vibrations of C=C were identified at 1559–1566 cm^{-1}. For C-H and CH_2, the peak at 1428–1439 cm^{-1} represented stretching vibrations in the aliphatics of biochars [52]. The band at 1088–1120 cm^{-1} was assigned to phenolic OH and aromatic C–O bonds. The weak vibrations of C–H bonds in the heteroaromatic and aromatic compounds were visible at 603–876 cm^{-1} [97,98]. The presence of polar groups, such as alcohol (OH), esters, ketones, aldehydes, carboxylic, ether, and phenols, suggests that the biochar samples may be useful as adsorbents for aqueous pollutants and as soil amendment to improve cation exchange [27,99].

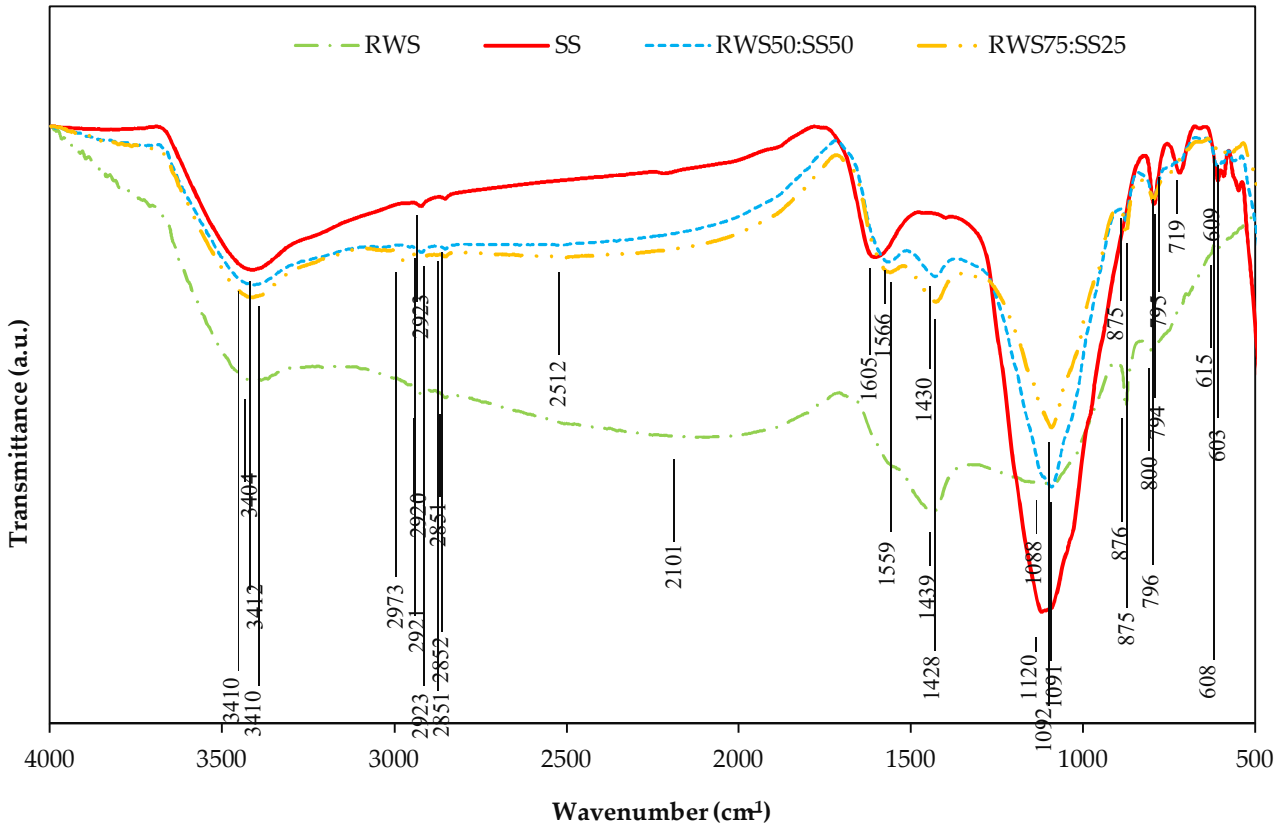

Figure 5. FTIR spectra of biochar samples.

3.2. Hydraulic Properties of Biochar

Figures 6 and 7 show the WHC and WRA of RWSB, SSB, and their blends (50:50 and 75:25) produced at 550 °C. The WHC was measured to be 1.01–3.08 (mL/g) as described by Ulusal et al. [48]. RWSB had a higher WHC than SSB or their co-blends, as shown in Figure 6. This study's biochars results were comparable with those in Zhang and You [100] and Reza et al. [10]. WHC, obtained by one-way ANOVA testing, is a significant indicator of the ability of biochar to hold moisture by cohesion and adhesion forces [47]. The surface area of biochar not only improves the WHC but also increases access to the functional groups, porous structure, and oxygen content [100]. The biochar with improved WHC is an effective adsorbent with micropores that can be saturated with water [101]. The biochar produced at a lower temperature has no more porosity than biochar produced at a higher temperature, and the water may not have access to the pores because of small pore volume, tar blocking the pores, and poor connectivity of the pores [102]. RWSB had a higher WHC than SSB and their blends (50:50 and 75:25). SSB has a solid sandy nature and contains very small pores and particles not more porous than RWSB (Figure 6).

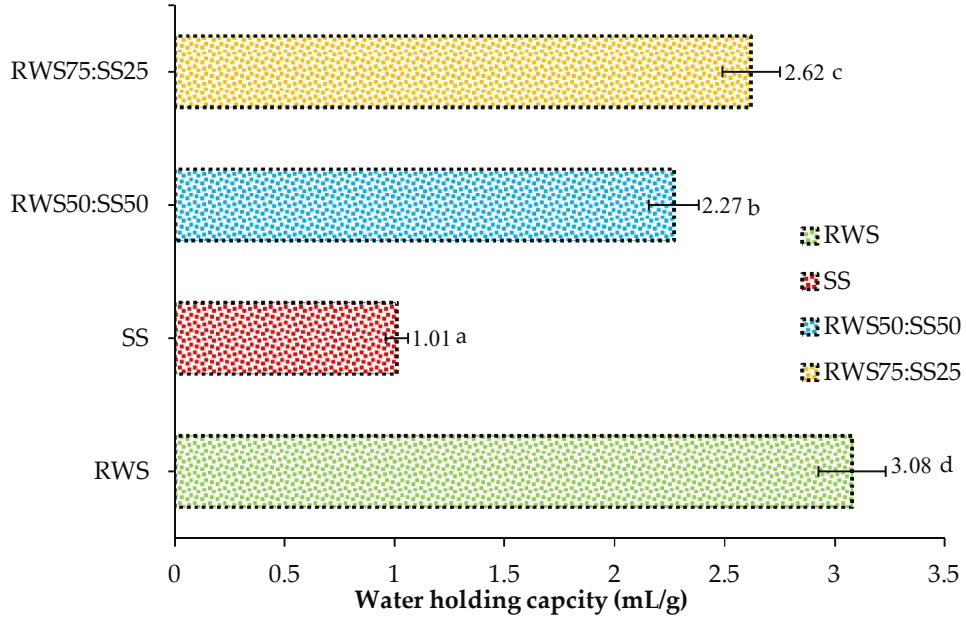

Figure 6. Water holding capacity of biochar samples. Data represent the averages and standard deviations based on triplicate experiments. Comparisons among the four treatments were significantly different and some same (Tukey, $p < 0.05$), and all the treatments are indicated by lowercase letters (a–d).

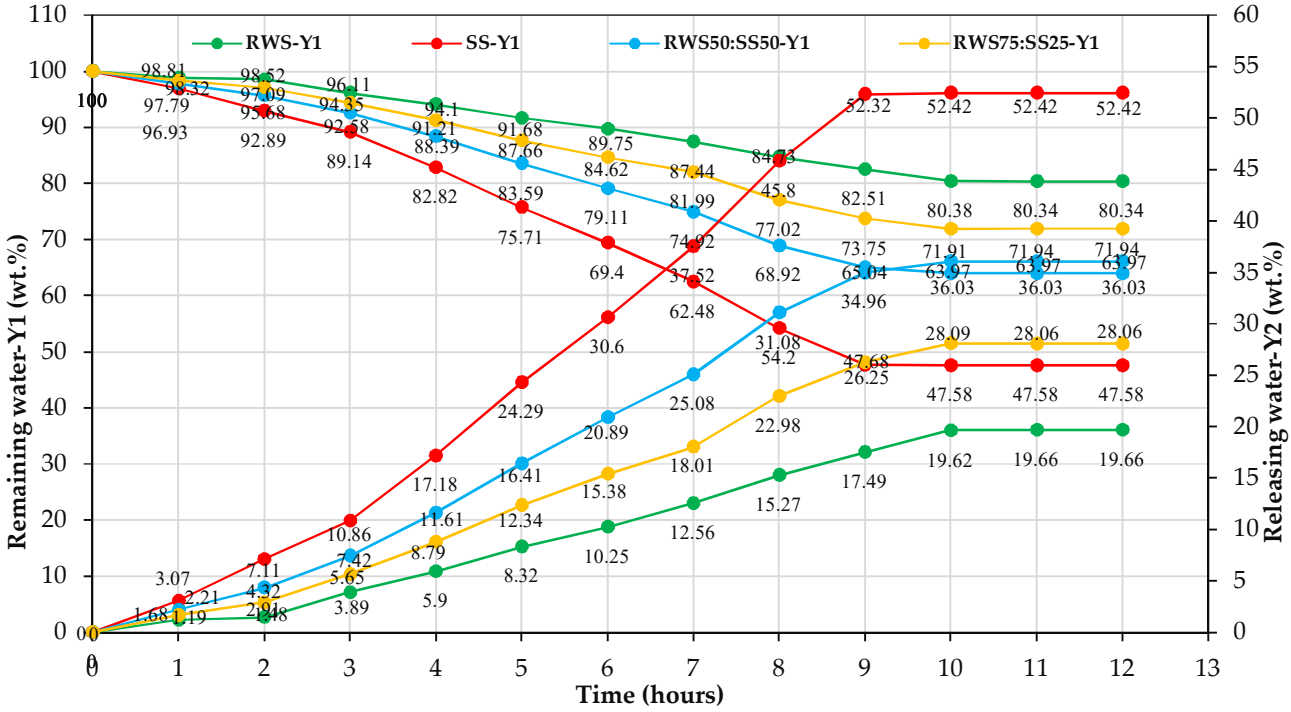

Figure 7. Water releasing and remaining behavior of biochar samples.

The WRA of RWSB, SSB, and their blend biochars (50:50 and 75:25) are shown in Figure 7. The WRA and remaining water results were in the ranges of 1.19–52.42 and 47.58–80.34 wt%, respectively. In the graphs, the symbol (-Y1) represents the remaining water and (-Y2) represents the released water from biochars. The present experiment allowed 12 h for the release of water until a constant weight was maintained. The released water (%) of RWSB was lower than that of SSB or the blends because its lower bulk density and larger micropore volume contributed to water retention [103]. The remaining water

(%) was opposite to the release of water (%) by biochars, and RWSB retained more water (%) than SSB or the blends. Biochar with a large pore volume and specific surface area is suitable for soil surface application to retain moisture over a prolonged period and to decrease the leaching of soil [104]. Among these tested biochars, RWSB showed high potential for filtration and for soil amendment because it has a large pore volume and specific surface areas for interactions with water.

4. Conclusions

This study investigated the characteristics of biochars produced from rubberwood sawdust (RWS), sewage sludge (SS), and their blends (50:50 and 75:25). The obtained results indicated that the SSB had high ash content (65.61 wt%) and low carbon content (24.27 wt%). Most of the components in SSB, including inorganic elements such as Si, Fe, K, Na, and P, were higher than those in RWSB and blended feedstock biochars. Despite this, co-pyrolysis of SS with RWS provided biochar with higher carbon content; however, the inorganic elements in this biochar also remained at high levels. SEM and BET results clearly showed that the surface of RWSB was more porous than that of SSB, whereas the surface area of SSB was higher than that of RWSB. The biochar with high porosity and surface area was determined to be feasible for applications such as soil amendment and biofilters. The obtained functional groups peaks of biochars were different, as observed from the FTIR results. The results of WHC and WRA of the biochars, including their pore properties and surface area, reveal their potential for adsorbent use in soil or water bodies. For biochar application as soil improvement, the biochar produced from RWS has more potential than SS or their blends (50:50 and 75:25) because it had a large pore volume, low bulk density, and high carbon content. SSB and blended biochars could be appropriately applied as soil nutrients to replace or substitute chemical fertilizers. Thus, these results will be helpful in the future to mitigate environmental pollution problems.

Author Contributions: Conceptualization, L.A. and A.P.; Formal analysis, L.A., A.P. and K.P.; Funding acquisition, K.P.; Investigation, L.A. and K.T.; Software editing, M.S.C.; Methodology, A.P. and K.T.; Project administration, K.P.; Resources, A.U.; Validation, A.U.; Writing—original draft, L.A.; Writing—review & editing, A.P., K.T., A.U. and K.P. All authors have read and agreed to the published version of the manuscript.

Funding: This research was supported from Prince of Songkla University and Ministry of Higher Education, Science, Research and Innovation under the Reinventing University Project (Grant Number REV64024).

Institutional Review Board Statement: Not applicable.

Informed Consent Statement: Not applicable.

Data Availability Statement: Not applicable.

Acknowledgments: This research was supported from Prince of Songkla University and Ministry of Higher Education, Science, Research and Innovation under the Reinventing University project (Grant Number REV64024). This manuscript has been language polished by native speaker from the Research and Development Office (RDO), Prince of Songkla University.

Conflicts of Interest: The authors declare no conflict of interest.

References

1. Li, Q.; Wang, M.; Fu, Q.; Li, T.; Liu, D.; Hou, R.; Li, H.; Cui, S.; Ji, Y. Short-term influence of biochar on soil temperature, liquid moisture content and soybean growth in a seasonal frozen soil area. *J. Environ. Manag.* **2020**, *266*, 110609. [CrossRef] [PubMed]
2. Lenderink, G.; van Ulden, A.; van den Hurk, B.; van Meijgaard, E. Summertime inter-annual temperature variability in an ensemble of regional model simulations: Analysis of the surface energy budget. *Clim. Chang.* **2007**, *81*, 233–247. [CrossRef]
3. Mulcahy, D.N.; Mulcahy, D.L.; Dietz, D. Biochar soil amendment increases tomato seedling resistance to drought in sandy soils. *J. Arid. Environ.* **2013**, *88*, 222–225. [CrossRef]
4. Finck, A. Fertilizer Use in African Agriculture. In *Lessons Learned and Good Practice Guidelines*; Morris, M., Kelley, V.A., Kopicki, R.J., Byerlee, D., Eds.; The World Bank: Washington, DC, USA, 2007; p. 144; ISBN 9-780821-368800.

5. Choi, Y.-K.; Jang, H.M.; Kan, E.; Wallace, A.R.; Sun, W. Adsorption of phosphate in water on a novel calcium hydroxide-coated dairy manure-derived biochar. *Environ. Eng. Res.* **2019**, *24*, 434–442. [CrossRef]
6. Novais, S.V.; Zenero, M.D.O.; Tronto, J.; Conz, R.F.; Cerri, C.E.P. Poultry manure and sugarcane straw biochars modified with MgCl2 for phosphorus adsorption. *J. Environ. Manag.* **2018**, *214*, 36–44. [CrossRef] [PubMed]
7. Xiang, A.; Qi, R.; Wang, M.; Zhang, K.; Jiang, E.; Ren, Y.; Hu, Z. Study on the infiltration mechanism of molten urea and biochar for a novel fertilizer preparation. *Ind. Crops Prod.* **2020**, *153*, 112558. [CrossRef]
8. Chen, L.; Wang, L.; Cho, D.-W.; Tsang, D.C.W.; Tong, L.; Zhou, Y.; Yang, J.; Hu, Q.; Poon, C.S. Sustainable stabilization/solidification of municipal solid waste incinerator fly ash by incorporation of green materials. *J. Clean. Prod.* **2019**, *222*, 335–343. [CrossRef]
9. Jung, K.-W.; Lee, S.; Lee, Y.J. Synthesis of novel magnesium ferrite ($MgFe_2O_4$)/biochar magnetic composites and its adsorption behavior for phosphate in aqueous solutions. *Bioresour. Technol.* **2017**, *245*, 751–759. [CrossRef] [PubMed]
10. Reza, M.S.; Afroze, S.; Bakar, M.S.A.; Saidur, R.; Aslfattahi, N.; Taweekun, J.; Azad, A.K. Biochar characterization of invasive Pennisetum purpureum grass: Effect of pyrolysis temperature. *Biochar* **2020**, *2*, 239–251. [CrossRef]
11. Lu, H.; Zhang, W.; Wang, S.; Zhuang, L.; Yang, Y.; Qiu, R. Characterization of sewage sludge-derived biochars from different feedstocks and pyrolysis temperatures. *J. Anal. Appl. Pyrolysis* **2013**, *102*, 137–143. [CrossRef]
12. Deng, B.; Yuan, X.; Siemann, E.; Wang, S.; Fang, H.; Wang, B.; Gao, Y.; Shad, N.; Liu, X.; Zhang, W.; et al. Feedstock particle size and pyrolysis temperature regulate effects of biochar on soil nitrous oxide and carbon dioxide emissions. *Waste Manag.* **2021**, *120*, 33–40. [CrossRef] [PubMed]
13. Schmidt, H.-P. *European Biochar Certificate (EBC)-Guidelines*; Version 6.1; European Biochar Certificate: Arbaz, Switzerland, 2015; Volume 2.
14. Basiri, N.; Fulcher, A.; Walker, F. *What Is Biochar and How Different Biochars Can Improve Your Crops*; University of Tennessee Institute of Agriculture: Knoxville, TN, USA, 2019.
15. Rodriguez, J.A.; Lustosa Filho, J.F.; Melo, L.C.A.; de Assis, I.R.; de Oliveira, T.S. Co-pyrolysis of agricultural and industrial wastes changes the composition and stability of biochars and can improve their agricultural and environmental benefits. *J. Anal. Appl. Pyrolysis* **2021**, *155*, 105036. [CrossRef]
16. Miyaoka, Y.; Yoochatchaval, W.; Sumino, H.; Banjongproo, P.; Yamaguchi, T.; Onodera, T.; Okadera, T.; Syutsubo, K. Evaluation of the process performance of a down-flow hanging sponge reactor for direct treatment of domestic wastewater in Bangkok, Thailand. *J. Environ. Sci. Health Part A* **2017**, *52*, 956–970. [CrossRef] [PubMed]
17. Parkpian, P.; Klankrong, K.; DeLaune, R.; Jugsujinda, A. Metal leachability from sewage sludge-amended Thai soils. *J. Environ. Sci. Health Part A* **2002**, *37*, 765–791. [CrossRef] [PubMed]
18. Phoungthong, K.; Suwunwong, T. Magnetic biochar derived from sewage sludge of concentrated natural rubber latex (CNRL) for the removal of Al^{3+} and Cu^{2+} ions from wastewater. *Res. Chem. Intermed.* **2020**, *46*, 385–407. [CrossRef]
19. Phoungthong, K.; Zhang, H.; Shao, L.-M.; He, P.-J. Leaching characteristics and phytotoxic effects of sewage sludge biochar. *J. Mater. Cycles Waste Manag.* **2018**, *20*, 2089–2099. [CrossRef]
20. Ruiz-Gómez, N.; Quispe, V.; Ábrego, J.; Atienza-Martínez, M.; Murillo, M.B.; Gea, G. Co-pyrolysis of sewage sludge and manure. *Waste Manag.* **2017**, *59*, 211–221. [CrossRef] [PubMed]
21. Wang, C.; Bi, H.; Lin, Q.; Jiang, X.; Jiang, C. Co-pyrolysis of sewage sludge and rice husk by TG–FTIR–MS: Pyrolysis behavior, kinetics, and condensable/non-condensable gases characteristics. *Renew. Energy* **2020**, *160*, 1048–1066. [CrossRef]
22. Rehman, R.A.; Rizwan, M.; Qayyum, M.F.; Ali, S.; Zia-ur-Rehman, M.; Zafar-ul-Hye, M.; Hafeez, F.; Iqbal, M.F. Efficiency of various sewage sludges and their biochars in improving selected soil properties and growth of wheat (*Triticum aestivum*). *J. Environ. Manag.* **2018**, *223*, 607–613. [CrossRef]
23. Wang, Z.; Tian, Q.; Guo, J.; Wu, R.; Zhu, H.; Zhang, H. Co-pyrolysis of sewage sludge/cotton stalks with K2CO3 for biochar production: Improved biochar porosity and reduced heavy metal leaching. *Waste Manag.* **2021**, *135*, 199–207. [CrossRef] [PubMed]
24. Yang, F.; Du, Q.; Sui, L.; Cheng, K. One-step fabrication of artificial humic acid-functionalized colloid-like magnetic biochar for rapid heavy metal removal. *Bioresour. Technol.* **2021**, *328*, 124825. [CrossRef]
25. Ali, L.; Palamanit, A.; Techato, K.; Baloch, K.A.; Jutidamrongphan, W. Valorization of rubberwood sawdust and sewage sludge by pyrolysis and co-pyrolysis using agitated bed reactor for producing biofuel or value-added products. *Environ. Sci. Pollut. Res.* **2021**, *29*, 1338–1363. [CrossRef] [PubMed]
26. Ali, L.; Ahmed Baloch, K.; Palamanit, A.; Raza, S.A.; Laohaprapanon, S.; Techato, K. Physicochemical Characterisation and the Prospects of Biofuel Production from Rubberwood Sawdust and Sewage Sludge. *Sustainability* **2021**, *13*, 5942. [CrossRef]
27. Li, S.; Chen, G. Thermogravimetric, thermochemical, and infrared spectral characterization of feedstocks and biochar derived at different pyrolysis temperatures. *Waste Manag.* **2018**, *78*, 198–207. [CrossRef] [PubMed]
28. Intani, K.; Latif, S.; Cao, Z.; Müller, J. Characterisation of biochar from maize residues produced in a self-purging pyrolysis reactor. *Bioresour. Technol.* **2018**, *265*, 224–235. [CrossRef]
29. Sakulkit, P.; Palamanit, A.; Dejchanchaiwong, R.; Reubroycharoen, P. Characteristics of pyrolysis products from pyrolysis and co-pyrolysis of rubber wood and oil palm trunk biomass for biofuel and value-added applications. *J. Environ. Chem. Eng.* **2020**, *8*, 104561. [CrossRef]
30. Mohan, D.; Pittman, C.U.; Steele, P.H. Pyrolysis of Wood/Biomass for Bio-oil: A Critical Review. *Energy Fuels* **2006**, *20*, 848–889. [CrossRef]

31. Remesh, P. Organic farming research in MP Organic farming in rain fed agriculture: Central institute for dry land agriculture. *Hyderabad* **2008**, 13–17.
32. Jeguirim, M.; Goddard, M.-L.; Tamosiunas, A.; Berrich-Betouche, E.; Azzaz, A.A.; Praspaliauskas, M.; Jellali, S. Olive mill wastewater: From a pollutant to green fuels, agricultural water source and bio-fertilizer. Biofuel production. *Renew. Energy* **2020**, *149*, 716–724. [CrossRef]
33. Dai, Z.; Meng, J.; Muhammad, N.; Liu, X.; Wang, H.; He, Y.; Brookes, P.C.; Xu, J. The potential feasibility for soil improvement, based on the properties of biochars pyrolyzed from different feedstocks. *J. Soils Sediments* **2013**, *13*, 989–1000. [CrossRef]
34. Novotny, E.H.; Maia, C.M.B.d.F.; Carvalho, M.T.d.M.; Madari, B.E. Biochar: Pyrogenic carbon for agricultural use-a critical review. *Rev. Bras. Ciênc. Solo* **2015**, *39*, 321–344. [CrossRef]
35. Oliveira, F.R.; Patel, A.K.; Jaisi, D.P.; Adhikari, S.; Lu, H.; Khanal, S.K. Environmental application of biochar: Current status and perspectives. *Bioresour. Technol.* **2017**, *246*, 110–122. [CrossRef]
36. Smith, P.; Adams, J.; Beerling, D.; Beringer, T.; Calvin, K.; Fuss, S.; Griscom, B.; Hagemann, N.; Kammann, C.; Kraxner, F.; et al. Impacts of Land-Based Greenhouse Gas Removal Options on Ecosystem Services and the United Nations Sustainable Development Goals. *Annu. Rev. Environ. Resour.* **2019**, *44*, 255–286. [CrossRef]
37. Gul, S.; Whalen, J.K.; Thomas, B.W.; Sachdeva, V.; Deng, H. Physico-chemical properties and microbial responses in biochar-amended soils: Mechanisms and future directions. *Agric. Ecosyst. Environ.* **2015**, *206*, 46–59. [CrossRef]
38. Sutradhar, I.; Jackson-deGraffenried, M.; Akter, S.; McMahon, S.A.; Waid, J.L.; Schmidt, H.-P.; Wendt, A.S.; Gabrysch, S. Introducing urine-enriched biochar-based fertilizer for vegetable production: Acceptability and results from rural Bangladesh. *Environ. Dev. Sustain.* **2021**, *23*, 12954–12975. [CrossRef]
39. Verheijen, F.; Jeffery, S.; Bastos, A.C.; Van der Velde, M.; Diafas, I. Biochar application to soils. *Crit. Sci. Rev. Eff. Soil Prop. Process. Funct. EUR* **2010**, *24099*, 162.
40. Enaime, G.; Baçaoui, A.; Yaacoubi, A.; Lübken, M. Biochar for Wastewater Treatment—Conversion Technologies and Applications. *Appl. Sci.* **2020**, *10*, 3492. [CrossRef]
41. Kongto, P.; Palamanit, A.; Chaiprapat, S.; Tippayawong, N. Enhancing the fuel properties of rubberwood biomass by moving bed torrefaction process for further applications. *Renew. Energy* **2021**, *170*, 703–713. [CrossRef]
42. Odeha, A.; Ogbeideb, S.; Okieimenc, C. Elucidation of the Influence of Coal Properties on Coal-Char Reactivity: A Look at Southern Hemisphere Coals. *J. Biosens. Bioelectron.* **2018**, *9*, 1–7. [CrossRef]
43. Krutof, A.; Bamdad, H.; Hawboldt, K.A.; MacQuarrie, S. Co-pyrolysis of softwood with waste mussel shells: Biochar analysis. *Fuel* **2020**, *282*, 118792. [CrossRef]
44. Harvey, O.R.; Kuo, L.-J.; Zimmerman, A.R.; Louchouarn, P.; Amonette, J.E.; Herbert, B.E. An Index-Based Approach to Assessing Recalcitrance and Soil Carbon Sequestration Potential of Engineered Black Carbons (Biochars). *Environ. Sci. Technol.* **2012**, *46*, 1415–1421. [CrossRef] [PubMed]
45. Choudhary, T.K.; Khan, K.S.; Hussain, Q.; Ahmad, M.; Ashfaq, M. Feedstock-induced changes in composition and stability of biochar derived from different agricultural wastes. *Arab. J. Geosci.* **2019**, *12*, 617. [CrossRef]
46. Palamanit, A.; Khongphakdi, P.; Tirawanichakul, Y.; Phusunti, N. Investigation of yields and qualities of pyrolysis products obtained from oil palm biomass using an agitated bed pyrolysis reactor. *Biofuel Res. J.* **2019**, *6*, 1065–1079. [CrossRef]
47. Song, W.; Guo, M. Quality variations of poultry litter biochar generated at different pyrolysis temperatures. *J. Anal. Appl. Pyrolysis* **2012**, *94*, 138–145. [CrossRef]
48. Ulusal, A.; Apaydın Varol, E.; Bruckman, V.J.; Uzun, B.B. Opportunity for sustainable biomass valorization to produce biochar for improving soil characteristics. *Biomass Convers. Biorefinery* **2020**, *11*, 1041–1051. [CrossRef]
49. Kabir, G.; Mohd Din, A.T.; Hameed, B.H. Pyrolysis of oil palm mesocarp fiber and palm frond in a slow-heating fixed-bed reactor: A comparative study. *Bioresour. Technol.* **2017**, *241*, 563–572. [CrossRef]
50. Nanda, S.; Dalai, A.K.; Berruti, F.; Kozinski, J.A. Biochar as an Exceptional Bioresource for Energy, Agronomy, Carbon Sequestration, Activated Carbon and Specialty Materials. *Waste Biomass Valorization* **2016**, *7*, 201–235. [CrossRef]
51. Diatta, A.A.; Fike, J.H.; Battaglia, M.L.; Galbraith, J.M.; Baig, M.B. Effects of biochar on soil fertility and crop productivity in arid regions: A review. *Arab. J. Geosci.* **2020**, *13*, 595. [CrossRef]
52. Bhattacharjee, N.; Biswas, A.B. Pyrolysis of Alternanthera philoxeroides (alligator weed): Effect of pyrolysis parameter on product yield and characterization of liquid product and bio char. *J. Energy Inst.* **2018**, *91*, 605–618. [CrossRef]
53. Dume, B.; Berecha, G.; Tulu, S. Characterization of biochar produced at different temperatures and its effect on acidic nitosol of Jimma, Southwest Ethiopia. *Int. J. Soil Sci.* **2015**, *10*, 63. [CrossRef]
54. Balashov, E.; Buchkina, N.; Šimanský, V.; Horák, J. Effects of slow and fast pyrolysis biochar on N_2O emissions and water availability of two soils with high water-filled pore space. *J. Hydrol. Hydromech.* **2021**, *69*, 467–474. [CrossRef]
55. Sahoo, S.S.; Vijay, V.K.; Chandra, R.; Kumar, H. Production and characterization of biochar produced from slow pyrolysis of pigeon pea stalk and bamboo. *Clean. Eng. Technol.* **2021**, *3*, 100101. [CrossRef]
56. Githinji, L. Effect of biochar application rate on soil physical and hydraulic properties of a sandy loam. *Arch. Agron. Soil Sci.* **2014**, *60*, 457–470. [CrossRef]
57. Shrivastava, P.; Kumar, A.; Tekasakul, P.; Lam, S.S.; Palamanit, A. Comparative Investigation of Yield and Quality of Bio-Oil and Biochar from Pyrolysis of Woody and Non-Woody Biomasses. *Energies* **2021**, *14*, 1092. [CrossRef]

58. Chakraborty, I.; Sathe, S.M.; Dubey, B.K.; Ghangrekar, M.M. Waste-derived biochar: Applications and future perspective in microbial fuel cells. *Bioresour. Technol.* **2020**, *312*, 123587. [CrossRef]
59. Rizwan, M.; Noureen, S.; Ali, S.; Anwar, S.; Rehman, M.Z.u.; Qayyum, M.F.; Hussain, A. Influence of biochar amendment and foliar application of iron oxide nanoparticles on growth, photosynthesis, and cadmium accumulation in rice biomass. *J. Soils Sediments* **2019**, *19*, 3749–3759. [CrossRef]
60. Wang, Y.; Liu, Y.; Zhan, W.; Zheng, K.; Wang, J.; Zhang, C.; Chen, R. Stabilization of heavy metal-contaminated soils by biochar: Challenges and recommendations. *Sci. Total Environ.* **2020**, *729*, 139060. [CrossRef] [PubMed]
61. Hassan, M.; Liu, Y.; Naidu, R.; Parikh, S.J.; Du, J.; Qi, F.; Willett, I.R. Influences of feedstock sources and pyrolysis temperature on the properties of biochar and functionality as adsorbents: A meta-analysis. *Sci. Total Environ.* **2020**, *744*, 140714. [CrossRef] [PubMed]
62. Wani, I.; Sharma, A.; Kushvaha, V.; Madhushri, P.; Peng, L. Effect of pH, Volatile Content, and Pyrolysis Conditions on Surface Area and O/C and H/C Ratios of Biochar: Towards Understanding Performance of Biochar Using Simplified Approach. *J. Hazard. Toxic Radioact. Waste* **2020**, *24*, 04020048. [CrossRef]
63. Usevičiūtė, L.; Baltrėnaitė-Gedienė, E. Dependence of pyrolysis temperature and lignocellulosic physical-chemical properties of biochar on its wettability. *Biomass Convers. Biorefinery* **2020**, *11*, 2775–2793. [CrossRef]
64. Wiedner, K.; Rumpel, C.; Steiner, C.; Pozzi, A.; Maas, R.; Glaser, B. Chemical evaluation of chars produced by thermochemical conversion (gasification, pyrolysis and hydrothermal carbonization) of agro-industrial biomass on a commercial scale. *Biomass Bioenergy* **2013**, *59*, 264–278. [CrossRef]
65. EBC, H. *European Biochar Certificate–Guidelines for a Sustainable Production of Biochar*; European Biochar Fondation (EBC): Arbaz, Switzerland, 2012.
66. Saleem, M.H.; Ali, S.; Rehman, M.; Hasanuzzaman, M.; Rizwan, M.; Irshad, S.; Shafiq, F.; Iqbal, M.; Alharbi, B.M.; Alnusaire, T.S.; et al. Jute: A Potential Candidate for Phytoremediation of Metals—A Review. *Plants* **2020**, *9*, 258. [CrossRef] [PubMed]
67. Deng, S.; Tan, H.; Wang, X.; Yang, F.; Cao, R.; Wang, Z.; Ruan, R. Investigation on the fast co-pyrolysis of sewage sludge with biomass and the combustion reactivity of residual char. *Bioresour. Technol.* **2017**, *239*, 302–310. [CrossRef]
68. Kończak, M.; Pan, B.; Ok, Y.S.; Oleszczuk, P. Carbon dioxide as a carrier gas and mixed feedstock pyrolysis decreased toxicity of sewage sludge biochar. *Sci. Total Environ.* **2020**, *723*, 137796. [CrossRef] [PubMed]
69. Huang, H.; Yang, T.; Lai, F.; Wu, G. Co-pyrolysis of sewage sludge and sawdust/rice straw for the production of biochar. *J. Anal. Appl. Pyrolysis* **2017**, *125*, 61–68. [CrossRef]
70. Jin, J.; Wang, M.; Cao, Y.; Wu, S.; Liang, P.; Li, Y.; Zhang, J.; Zhang, J.; Wong, M.H.; Shan, S.; et al. Cumulative effects of bamboo sawdust addition on pyrolysis of sewage sludge: Biochar properties and environmental risk from metals. *Bioresour. Technol.* **2017**, *228*, 218–226. [CrossRef] [PubMed]
71. Wei, S.; Zhu, M.; Fan, X.; Song, J.; Peng, P.; Li, K.; Jia, W.; Song, H. Influence of pyrolysis temperature and feedstock on carbon fractions of biochar produced from pyrolysis of rice straw, pine wood, pig manure and sewage sludge. *Chemosphere* **2019**, *218*, 624–631. [CrossRef] [PubMed]
72. Khalid, S.; Shahid, M.; Murtaza, B.; Bibi, I.; Natasha; Asif Naeem, M.; Niazi, N.K. A critical review of different factors governing the fate of pesticides in soil under biochar application. *Sci. Total Environ.* **2020**, *711*, 134645. [CrossRef] [PubMed]
73. Zhou, C.; Zhang, Y.; Liu, Y.; Deng, Z.; Li, X.; Wang, L.; Dai, J.; Song, Y.; Jiang, Z.; Qu, J.; et al. Co-pyrolysis of textile dyeing sludge and red wood waste in a continuously operated auger reactor under microwave irradiation. *Energy* **2021**, *218*, 119398. [CrossRef]
74. Huang, H.; Reddy, N.G.; Huang, X.; Chen, P.; Wang, P.; Zhang, Y.; Huang, Y.; Lin, P.; Garg, A. Effects of pyrolysis temperature, feedstock type and compaction on water retention of biochar amended soil. *Sci. Rep.* **2021**, *11*, 7419. [CrossRef]
75. Hamza, U.D.; Nasri, N.S.; Amin, N.S.; Mohammed, J.; Zain, H.M. Characteristics of oil palm shell biochar and activated carbon prepared at different carbonization times. *Desalination Water Treat.* **2016**, *57*, 7999–8006. [CrossRef]
76. Kim, K.H.; Kim, J.-Y.; Cho, T.-S.; Choi, J.W. Influence of pyrolysis temperature on physicochemical properties of biochar obtained from the fast pyrolysis of pitch pine (*Pinus rigida*). *Bioresour. Technol.* **2012**, *118*, 158–162. [CrossRef] [PubMed]
77. Oja, V.; Hajaligol, M.R.; Waymack, B.E. The vaporization of semi-volatile compounds during tobacco pyrolysis. *J. Anal. Appl. Pyrolysis* **2006**, *76*, 117–123. [CrossRef]
78. Mohanty, P.; Nanda, S.; Pant, K.K.; Naik, S.; Kozinski, J.A.; Dalai, A.K. Evaluation of the physiochemical development of biochars obtained from pyrolysis of wheat straw, timothy grass and pinewood: Effects of heating rate. *J. Anal. Appl. Pyrolysis* **2013**, *104*, 485–493. [CrossRef]
79. Yuan, J.-H.; Xu, R.-K.; Zhang, H. The forms of alkalis in the biochar produced from crop residues at different temperatures. *Bioresour. Technol.* **2011**, *102*, 3488–3497. [CrossRef]
80. Al-Wabel, M.I.; Al-Omran, A.; El-Naggar, A.H.; Nadeem, M.; Usman, A.R.A. Pyrolysis temperature induced changes in characteristics and chemical composition of biochar produced from conocarpus wastes. *Bioresour. Technol.* **2013**, *131*, 374–379. [CrossRef] [PubMed]
81. Angın, D. Effect of pyrolysis temperature and heating rate on biochar obtained from pyrolysis of safflower seed press cake. *Bioresour. Technol.* **2013**, *128*, 593–597. [CrossRef] [PubMed]
82. Ferreira, S.D.; Manera, C.; Silvestre, W.P.; Pauletti, G.F.; Altafini, C.R.; Godinho, M. Use of Biochar Produced from Elephant Grass by Pyrolysis in a Screw Reactor as a Soil Amendment. *Waste Biomass Valorization* **2019**, *10*, 3089–3100. [CrossRef]

83. Han, Q.; Yang, Y.; Wang, R.; Zhang, K.; Liu, N.; Hong, M. Biochar Derived from Agricultural Wastes as a Means of Facilitating the Degradation of Azo Dyes by Sulfides. *Catalysts* **2021**, *11*, 434. [CrossRef]
84. Duku, M.H.; Gu, S.; Hagan, E.B. Biochar production potential in Ghana—A review. *Renew. Sustain. Energy Rev.* **2011**, *15*, 3539–3551. [CrossRef]
85. Chan, K.Y.; Zwieten, L.V.; Meszaros, I.; Downie, A.; Joseph, S.; Chan, K.Y.; Zwieten, L.V.; Meszaros, I.; Downie, A.; Joseph, S. Agronomic values of greenwaste biochar as a soil amendment. *Soil Res.* **2007**, *45*, 629–634. [CrossRef]
86. Spokas, K.A.; Koskinen, W.C.; Baker, J.M.; Reicosky, D.C. Impacts of woodchip biochar additions on greenhouse gas production and sorption/degradation of two herbicides in a Minnesota soil. *Chemosphere* **2009**, *77*, 574–581. [CrossRef] [PubMed]
87. Worasuwannarak, N.; Sonobe, T.; Tanthapanichakoon, W. Pyrolysis behaviors of rice straw, rice husk, and corncob by TG-MS technique. *J. Anal. Appl. Pyrolysis* **2007**, *78*, 265–271. [CrossRef]
88. Zimmerman, A.R. Abiotic and Microbial Oxidation of Laboratory-Produced Black Carbon (Biochar). *Environ. Sci. Technol.* **2010**, *44*, 1295–1301. [CrossRef]
89. Ahmad, M.; Lee, S.S.; Dou, X.; Mohan, D.; Sung, J.-K.; Yang, J.E.; Ok, Y.S. Effects of pyrolysis temperature on soybean stover- and peanut shell-derived biochar properties and TCE adsorption in water. *Bioresour. Technol.* **2012**, *118*, 536–544. [CrossRef] [PubMed]
90. Yin, Q.; Liu, M.; Ren, H. Biochar produced from the co-pyrolysis of sewage sludge and walnut shell for ammonium and phosphate adsorption from water. *J. Environ. Manag.* **2019**, *249*, 109410. [CrossRef]
91. Karimi, A.; Naghizadeh, A.; Biglari, H.; Peirovi, R.; Ghasemi, A.; Zarei, A. Assessment of human health risks and pollution index for heavy metals in farmlands irrigated by effluents of stabilization ponds. *Environ. Sci. Pollut. Res.* **2020**, *27*, 10317–10327. [CrossRef] [PubMed]
92. Agrafioti, E.; Bouras, G.; Kalderis, D.; Diamadopoulos, E. Biochar production by sewage sludge pyrolysis. *J. Anal. Appl. Pyrolysis* **2013**, *101*, 72–78. [CrossRef]
93. Fidel, R.B.; Laird, D.A.; Thompson, M.L.; Lawrinenko, M. Characterization and quantification of biochar alkalinity. *Chemosphere* **2017**, *167*, 367–373. [CrossRef]
94. Mukherjee, R.; Paul, T.; Soren, J.P.; Halder, S.K.; Mondal, K.C.; Pati, B.R.; Das Mohapatra, P.K. Acidophilic α-Amylase Production from Aspergillus niger RBP7 Using Potato Peel as Substrate: A Waste to Value Added Approach. *Waste Biomass Valorization* **2019**, *10*, 851–863. [CrossRef]
95. Camargo, D.; Sene, L. Production of ethanol from the hemicellulosic fraction of sunflower meal biomass. *Biomass Convers. Biorefinery* **2014**, *4*, 87–93. [CrossRef]
96. Gupta, G.K.; Ram, M.; Bala, R.; Kapur, M.; Mondal, M.K. Pyrolysis of chemically treated corncob for biochar production and its application in Cr(VI) removal. *Environ. Prog. Sustain. Energy* **2018**, *37*, 1606–1617. [CrossRef]
97. Elnour, A.Y.; Alghyamah, A.A.; Shaikh, H.M.; Poulose, A.M.; Al-Zahrani, S.M.; Anis, A.; Al-Wabel, M.I. Effect of Pyrolysis Temperature on Biochar Microstructural Evolution, Physicochemical Characteristics, and Its Influence on Biochar/Polypropylene Composites. *Appl. Sci.* **2019**, *9*, 1149. [CrossRef]
98. Zolfi Bavariani, M.; Ronaghi, A.; Ghasemi, R. Influence of Pyrolysis Temperatures on FTIR Analysis, Nutrient Bioavailability, and Agricultural use of Poultry Manure Biochars. *Commun. Soil Sci. Plant Anal.* **2019**, *50*, 402–411. [CrossRef]
99. Stella Mary, G.; Sugumaran, P.; Niveditha, S.; Ramalakshmi, B.; Ravichandran, P.; Seshadri, S. Production, characterization and evaluation of biochar from pod (*Pisum sativum*), leaf (*Brassica oleracea*) and peel (*Citrus sinensis*) wastes. *Int. J. Recycl. Org. Waste Agric.* **2016**, *5*, 43–53. [CrossRef]
100. Zhang, J.; You, C. Water Holding Capacity and Absorption Properties of Wood Chars. *Energy Fuels* **2013**, *27*, 2643–2648. [CrossRef]
101. Gray, M.; Johnson, M.G.; Dragila, M.I.; Kleber, M. Water uptake in biochars: The roles of porosity and hydrophobicity. *Biomass Bioenergy* **2014**, *61*, 196–205. [CrossRef]
102. Das, O.; Sarmah, A.K. The love–hate relationship of pyrolysis biochar and water: A perspective. *Sci. Total Environ.* **2015**, *512–513*, 682–685. [CrossRef]
103. Shaaban, A.; Se, S.-M.; Mitan, N.M.M.; Dimin, M.F. Characterization of Biochar Derived from Rubber Wood Sawdust through Slow Pyrolysis on Surface Porosities and Functional Groups. *Procedia Eng.* **2013**, *68*, 365–371. [CrossRef]
104. Lehmann, J.; Gaunt, J.; Rondon, M. Bio-char Sequestration in Terrestrial Ecosystems—A Review. *Mitig. Adapt. Strateg. Glob. Chang.* **2006**, *11*, 403–427. [CrossRef]